Organic & Biomolecular Chemistry

PAPER

Cite this: *Org. Biomol. Chem.*, 2017, **15**, 4135

Changing the path of least resistance, or access to *endo*-dig products *via* a sequence of three *exo*-trig transition states: electronic effects in homoallylic ring expansion cascades of alkenyl isonitriles†

Gabriel dos Passos Gomes, ‡ Christopher J. Evoniuk,‡ Michelle Ly and Igor V. Alabugin*

Received 2nd March 2017,
Accepted 3rd April 2017

DOI: 10.1039/c7ob00527j

rsc.li/obc

Chemoselective addition of radicals to isonitriles can be harnessed for initiating reaction cascades designed to overcome the stereoelectronic restrictions on homoallylic ring expansion in alkyne reactions and to develop a new general route for the preparation of N-heteroaromatics. This method utilizes alkenes as synthetic equivalents of alkynes by coupling homoallylic ring expansion to yield the formal "6-*endo*" products with aromatization *via* stereoelectronically assisted C–C bond scission. Detailed computational analysis of the individual steps of the homoallylic expansion sequence maps effects of substituents and structural constraints on this multi-step potential energy surface.

Cyclization reactions of alkene and alkynes have two possible regiochemical outcomes. Nucleophilic and radical attack at the internal atom of the π-bond (*i.e.*, the *exo*-attack) is generally more stereoelectronically favored and kinetically preferred in comparison to the alternative *endo*-attack at the external atom of the π-bond (Scheme 1). This kinetic preference is often observed even when the *endo*-products are more stable thermodynamically, *e.g.*, due to a larger size of the formed cycle.

Ring expansions allow us to overcome stereoelectronic restrictions associated with inefficiency of unfavorable *endo*-cyclizations and form the *endo*-products *via* an alternative route that starts from the initially formed *exo*-trig products. Generally, the expansion sequences transform the latter *via* two additional steps, *i.e.*, cyclization and fragmentation. An interesting feature of the penultimate and ultimate steps of this sequence is that both of them proceed *via* a formally *exo* transition state (TS), *i.e.*, as a 3-*exo*-trig and a retro-3-*exo*-trig process (Scheme 1).

Such expansion, rendered possible by the presence of an adjacent π-bond and the intrinsically low barriers of radical 3-*exo* cyclizations, has been implicated in a variety of radical

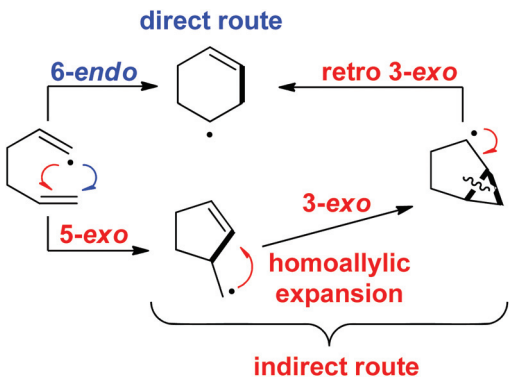

Scheme 1 Direct and indirect (*i.e.*, the homoallylic ring expansion (HRE)) routes to the *endo*-products formed from vinyl radicals.

rearrangements. We have recently established a combination of Bu_3Sn-mediated 5-*exo*-trig cyclization of enynes with homoallylic ring expansion (HRE)[1,2] and C–C fragmentation as an indirect but efficient way to six-membered aromatic compounds that are inaccessible from the 6-*endo*-dig cyclization of related bis-alkynes (Scheme 2).[3]

The combination of HRE and C–C scission opens a way to bypass synthetic limitations on the feasibility of 6-*endo*-dig cyclizations imposed by the electronic structure of alkyne functionality. Although the 6-*endo*-dig ring closure is the most direct route for the preparation of polycyclic aromatic hydrocarbons (PAHs) from alkynes, the stereoelectronically preferred

Department of Chemistry and Biochemistry, Florida State University, Tallahassee, Florida 32306-4390, USA. E-mail: alabugin@chem.fsu.edu

† Electronic supplementary information (ESI) available: Experimental procedures and compound characterization data (PDF). See DOI: 10.1039/c7ob00527j

‡ These authors contributed equally to this work. All authors have given approval to the final version of the manuscript.

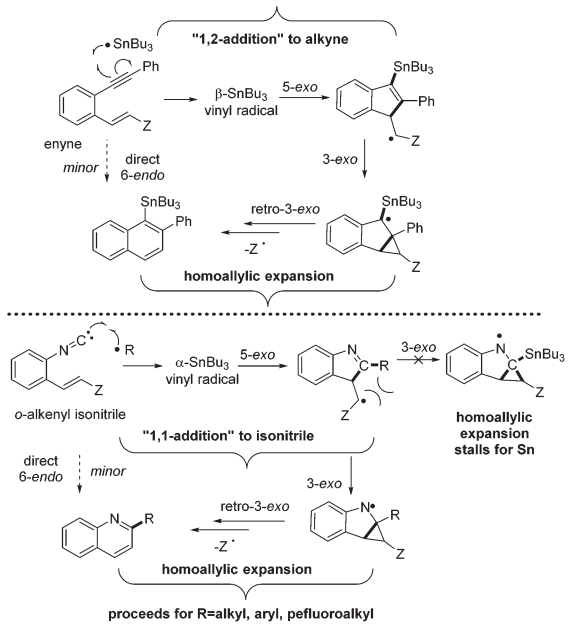

Scheme 2 Two application of alkenes as alkyne equivalents in radical cascades terminated by fragmentation. Top: All carbon system allows for HRE process with using AIBN/HSnBu$_3$. Bottom: α-SnBu$_3$ substituent prevents HRE in isonitrile system but aryl, alkyl and perfluoroalkyl groups do not.

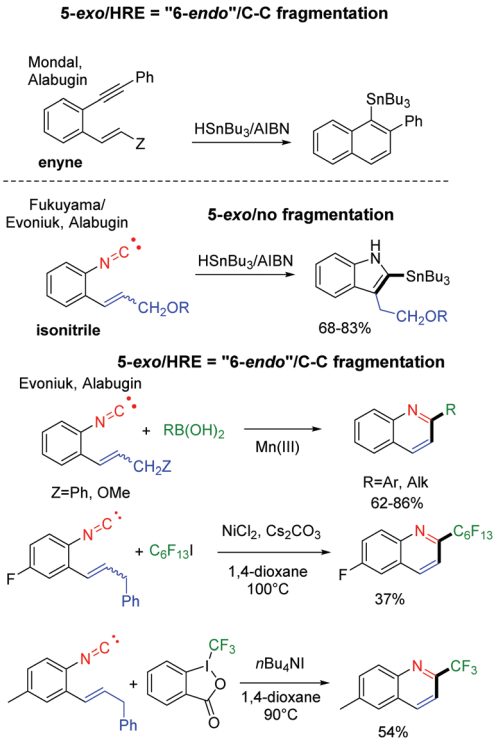

Scheme 3 Contrasting selectivities of enyne and isonitrile reactions promoted by different radical sources.

5-*exo*-dig path often dominates in the radical version of this process.[4]

Two conditions are important for the success of this transformation where alkenes are used as synthetic equivalents of alkynes in order to bypass the unreliable *endo*-dig cyclization. One of them is the design of radical leaving groups which should contain bonds sufficiently strong to be compatible with the radical conditions, but undergo fast scission at the end of cascade.[3a] The second important design condition is ensuring that the reaction does not stop at the initially formed 5-*exo*-trig product. The latter should be capable of 3-*exo*-trig cyclization that initiates HRE *via* the formation of a relatively strained intermediate. We found that this stage of the cascade is sensitive to the nature of reactants. Experimental work from the literature[1,2] and from our group[3,5] suggested that the 5-*exo*-trig/HRE sequence can be interrupted at different stages (Scheme 3).

For example, we found only the 5-*exo* indole products in the reactions of HSnBu$_3$/AIBN with *o*-alkenylarylisonitriles (Scheme 3). This finding is consistent with the earlier literature report of Fukuyama and coworkers who found that the initial 5-*exo*-products do not undergo the ring expansion even for alkyl substituted alkenes where the highly reactive 5-*exo* radical intermediates are formed that are were not deactivated by resonance stabilization.[6a] The results of this thorough study contrast drastically with our observation of efficient ring-expansion/fragmentation cascades in the analogous all-carbon systems.[3]

Our hypothesis was that the variation in selectivity stems from the difference in the position of the bulky Bu$_3$Sn group relative to the radical center in the two types of vinyl radicals.[7] The Bu$_3$Sn addition to enynes forms a β-Sn-substituted radical where bulky –SnBu$_3$ moiety is placed *away* from the point of the new bond formation in the subsequent 3-*exo*-step (Scheme 2). This radical readily undergoes the HRE process because the 3-*exo*-cyclization TS is not sterically hindered. In contrast, isonitriles act as a "1,1-synthon" in radical additions, to form an α-Sn-substituted iminoyl radical. Consequently, the initial product of the 5-*exo* cyclization of isonitrile has the bulky SnBu$_3$-group directly at the radical carbon involved in the initiation of subsequent HRE. The increased steric hindrance should slow the 3-*exo*-step of sequence, explaining why the HRE cascade stops and only the indole products are observed (Scheme 2).

Guided by this hypothesis we expanded this work to other, less bulky radical sources and found that the above mentioned lack of HRE is not general and that metal-mediated reactions of organoboron reagents that are believed to generate aryl and alkyl radicals *via* oxidative approaches[8–10] led to the smooth formation of formal 6-*endo*-products.[5] The "6-*endo*" product **5c** formation was observed exclusively when an appropriate fragmenting group (*i.e.*, CH$_2$Ph, –CH$_2$OMe) was installed. Furthermore, the same 6-*endo*-selectivity was observed in radical perfluoroalkylations, providing an interesting contrast to analogous reactions of similar systems.[11,12]

Potentially, the *endo*-products produced in these new systems can be either produced directly or formed *via* HRE of the 5-*exo*-trig radical **A3**. The goal of this paper was to under-

stand the role of substituents in determining the scope and limitations of HRE in a quantitative manner, thus paving the way for the development of future cascade reactions. The complementary goal was to test for the possibility of changing intrinsic preferences by using structural constrains such as additionally annealed cycles.

Computational analysis

Calculations were carried out with the Gaussian 09 software package,[13] using the M06-2X DFT functional,[14] previously shown to provide a good description of thermodynamics and kinetics for radical cascade reactions.[15] We used the 6-311++G (d,p) basis set for all atoms except of Sn, for which we opted for the Def2-QZVP[16] basis set. The implicit PCM[17] solvation model was used to simulate the effects of toluene throughout the reaction pathways. We also performed Natural Bond Orbital[18] (NBO) analysis on key intermediates and transition states.

These computational tools were used to understand the mechanistic questions; whose interplay was responsible for the efficiency of the observed pathways. After evaluating the 5-*exo vs.* 6-*endo* selectivity of the initial ring closure, we also investigated the effect of attacking radicals the feasibility of the 3-*exo* cyclization, the gateway step for HRE. We also provided the general analysis of the full potential energy surfaces for the overall multi-step transformation.

Substituent effects on the structure of imidoyl radicals

Although vinyl and imidoyl radical are isoelectronic, these species are not as similar as one would expect. For example, aryl-substituted vinyl radicals are fully conjugated with the aryl group, with the spin density delocalized and nearly linear geometry (CCC angle ~180°) that holds the radical center in a p-orbital. Imidoyl radicals, on the other hand, are heavily localized with a $sp^{2.4}$-hybridized radical orbital. Consequently, even the Ph-substituted radicals of the latter type adopt a bent geometry (NCC angle ~130°, Scheme 4) which is perfect for cascade cyclizations. In contrast with the Ph-substituted vinyl radical, the Ph π-system is not conjugated with the radical center. We attribute this dichotomy to a strong 2c,3e interaction between nitrogen's lone pair and the radical center in the imidoyl radical.[19] Interaction with the lone pair provides significant stabilization to the radical center. Since the radical center is already stabilized, the C-terminal Ph ring prefers to be aligned instead with the out-of-plane π-system of the N=C moiety. The fully planar conformation is higher in energy, albeit only marginally (ΔH = 0.3 kcal mol^{-1}, ΔG = 0.6 kcal mol^{-1}).[20]

Substitution at the radical center affects orbital hybridization and geometry at this position. For example, the $SnMe_3$-group increases the NCR angle. In contrast, the CF_3 group increased bending, s-character and electrophilicity at the radical center (Scheme 5). Several other structural features are interesting. Whereas the lone pair of nitrogen and the radical orbital are always aligned perfectly (indicating the presence of a strong 2c,3e-bond between these non-bonding centers) the C_{Ar}–C_{Ar}–C–N dihedrals vary. Interestingly, neither the lone pair of nitrogen nor the N=C π-bond are perfectly aligned with the central aromatic π-system for all four radicals in Scheme 5. The Sn-substituted reactant is the most twisted (C–C–N–C dihedral of ~57 degrees) whereas the C-substituted systems are closer to planarity. Steric effects are obviously important in shaping the non-planar arrangement of conjugating substituents at the aromatic core. The alkene π-bond is nearly orthogonal to the aromatic cloud for R = $SnMe_3$ and CF_3, adopting a nearly perfect orientation for the intramolecular radical attack, so no loss of conjugation between alkene and the central aromatic ring is needed to reach the near-attack conformation.

On other hand, the delocalizing interactions with substituents at the radical terminus are maximized by nearly optimal geometries for the hyperconjugative (where radical is antiperiplanar to Sn–C, C–H, and C–F bonds, respectively for **1a,b,d** [21]) or conjugative (C=N moiety aligned with the terminal Ph group in **1c**) interactions of the radical center. These interactions also do not have to be sacrificed for reaching the near-attack arrangement of the radical and the target alkene.

5-*exo vs.* 6-*endo*. In the next step, we applied computational analysis to understand the competition between 5-*exo vs.* 6-*endo*-trig cyclizations (Scheme 6). For the parent system, the DFT barriers clearly favor the 5-*exo*-path. For example, in the Me-substituted system the 5-*exo* barrier is almost 6 kcal mol^{-1}

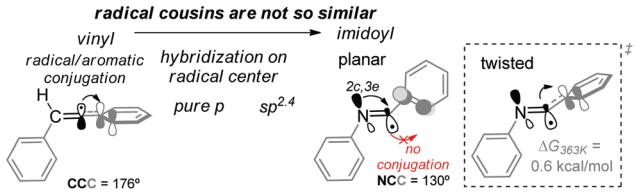

Scheme 4 Comparison of Ph-substituted vinyl and imidoyl radicals.

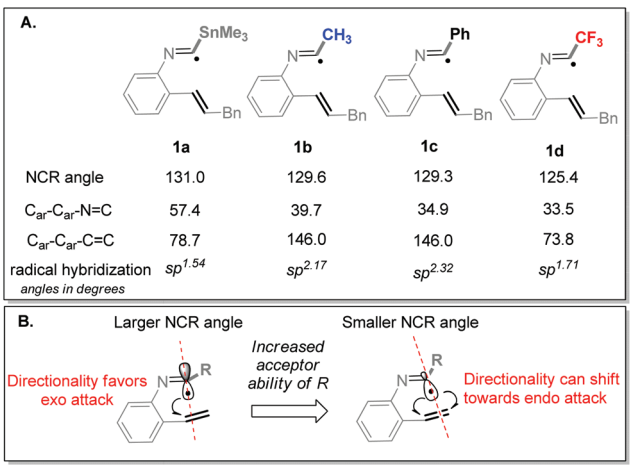

Scheme 5 Substituent effects on the structure of imidoyl radicals and expected consequences for the radical reactivity.

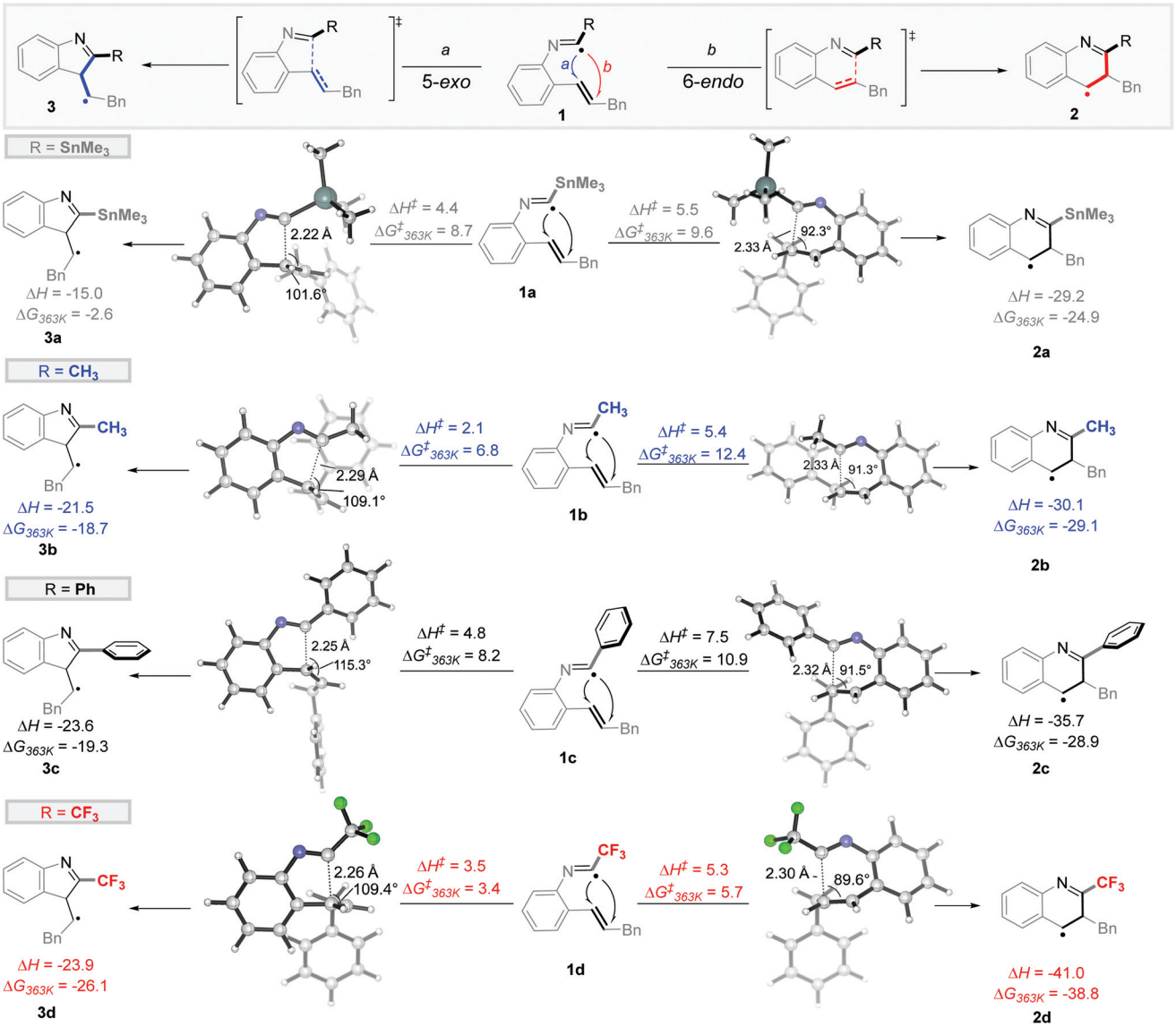

Scheme 6 Influence of adjacent groups on 5-*exo vs.* 6-*endo* cyclizations, energies in kcal mol^{-1}.

lower than the 6-*endo* barrier (6.8 *vs.* 12.4 kcal mol^{-1}) even though the 6-*endo* ring closure is ~10 kcal mol^{-1} more exergonic (5-*exo*: −19 kcal mol^{-1} *vs.* 6-*endo*: −29 kcal mol^{-1}). In both transition states, the alkene moiety is rotated orthogonally to the *endo*-cyclic benzene π-system and, thus, cannot benefit from conjugation with the latter.

The kinetic preference for the *exo*-cyclization reflects the fundamental stereoelectronic preferences for the bond formation.[22] Selected TS geometries shown in Scheme 6 illustrate that the attack angle for the 5-*exo* TS is much closer to the obtuse Burgi–Dunitz trajectory (preferred for the unconstrained intermolecular radical additions to alkenes). In contrast, the 6-*endo*-trig attack angles are close to 90 degrees. It is also interesting the attack angle in the 5-*exo* TS varies much more widely (from 102 to 115 degrees) whereas the 6-*endo* attack is more constrained (90–92 degrees).

The smallest attack angle was found in the 6-*endo* TS for the most electrophilic CF_3-substituted radical. This angle of 89.6 degrees corresponds to the only formally acute angle of attack. Such small angle of attack is usually forced by geometric constraints in nucleophilic closures of small cycles or by electronic features of electrophilic cyclizations (or electrophile-assisted nucleophilic cyclizations).[21]

We have also evaluated the effects of additional structural constraints in the alkene on the 5-*exo*/6-*endo*-trig competition (Scheme 7). Annealing the alkene moiety into a five-membered ring has dramatic effect on the relative magnitude of the cyclization barriers (5-*exo*: 5.5 kcal mol^{-1} *vs.* 6-*endo*: 5.3 kcal mol^{-1}), rendering the *endo*-trig path to be slightly kinetically favorable.

Superficially, this trend may seem like a reflection of additional strain imposed by the presence of two five-mem-

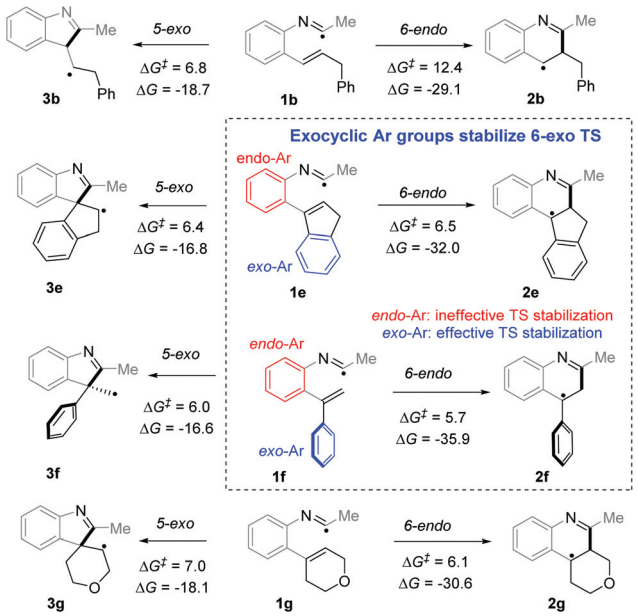

Scheme 7 Substrate comparison for 6-*endo vs.* 5-*exo* pathways, energies in kcal mol^{-1}.

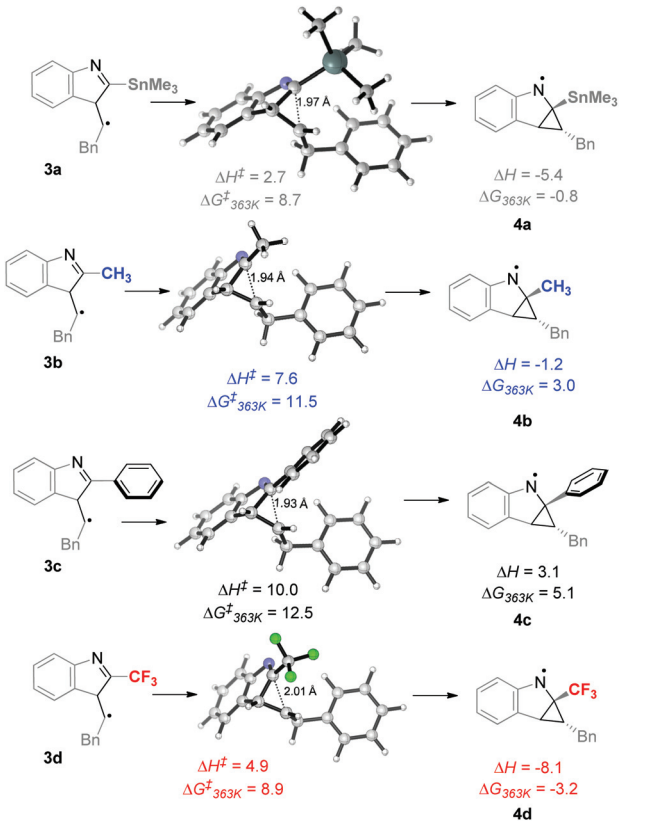

Scheme 8 Substrate comparison for 3-*exo* cyclization. Adjacent group can influence this step through steric or electronic effects.

bered rings in the 5-*exo*-product, an effect that is well-known when the five-membered rings are *fused* together.[23,24] However, the lack of increase in the 5-*exo* barrier suggests that strain is *un*important in changing the *exo*/*endo* balance in this system. Furthermore, the two five-membered rings are not fused and share only one atom (the spiro-connection). The answer to the strong acceleration of the 6-*endo*-pathway in this case is stabilization of the 6-*endo* TS. Unlike the tricyclic 6-*endo* radical **2b** (Scheme 7), the tetracyclic 6-*endo*-radical **2a** (Scheme 7) benefits from benzylic conjugation from an *exo*-aryl group. Dramatic decrease in the 6-*endo*-barrier suggests that this stabilizing effect is already in action at the TS stage. Of course, in the absence of any restraints, an *exo* Ph group is even more effective (5.7 kcal mol^{-1} barrier for the 6-*endo*-cyclization to form radical **2b**). Interestingly, even fusion to a saturated cycle can be sufficient for changing the 5-*exo*/6-*endo* balance as illustrated by the last example in Scheme 7.

3-*exo*-step. It is also instructive to compare the effect of α-substitution on the reactivity of α-imidoyl radicals in the first step of ring expansion (HRE). This step is mildly endergonic for the Ph and Me substituents but exergonic for CF_3 (Scheme 8). The differences in the reaction energies indicated different patterns of stabilization that substituents impose on the reactant and product. Comparison of geometries, barriers, and reaction energies illustrated that $SnMe_3$ is similar to Me and Ph in its effect on reactivity. The more negative reaction exergonicity is associated with an earlier TS and a lower barrier for these systems.

Interestingly, the 3-*exo*-trig closure of a $SnMe_3$ substituted radical is also exergonic and fast within the present computational model (Schemes 8 and 9). The $SnMe_3$ group (*i.e.*, the truncated version of $SnBu_3$ radical) does not stop the 3-*exo-trig* closure, suggesting that the lack of HRE in Bu_3Sn-mediated enyne cyclizations results from a steric rather than an electronic effect. Although the size and conformational complexity of the full $SnBu_3$ radical precluded us from using it in the computational studies, the computed TS geometry for the **3a** → **4a** transformation makes it clear the change from $SnMe_3$ to $SnBu_3$ radical in the 3-*exo* TS will lead to significant steric strain. On the other hand, the CF_3 case is different: the activation barrier is higher than one would expect from the relative free energies of the cyclization and along with the later TS, it is suggestive of the acceptor group deactivating the imine moiety towards the radical attack (Scheme 9).

The retro 3-*exo*-step. Computational results for this step are summarized below in Scheme 10. Although the process is generally thermodynamically favourable, the activation barriers for this step are relatively high. These barriers range from ~14 to 20 kcal mol^{-1}, depending on the substituent. The misconnect between kinetics and thermodynamics originates from the relatively poor overlap between the breaking bond and the radical center. Interestingly, the acceptor CF_3 group increases the barrier and the respective ring opening is the least exergonic. On the other hand, the π-conjugating Ph group decreases the barrier, likely due to its ability to assist in the *endo* C–C bond scission as illustrated by alignment of this ring with the breaking bond in the TS (Scheme 10).

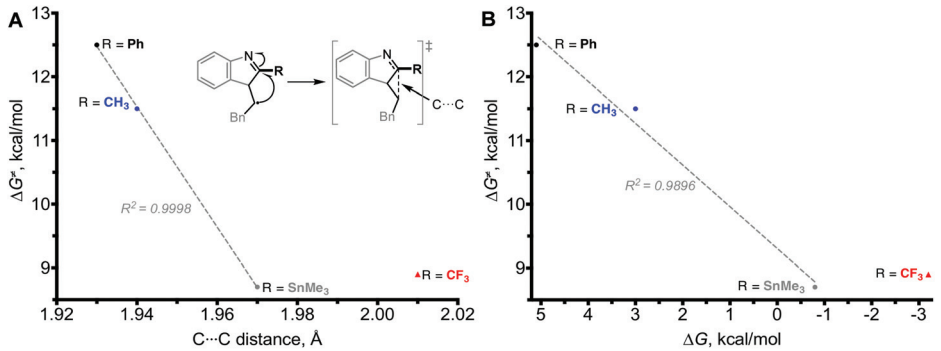

Scheme 9 Unusual effect of CF_3-substituent on the 3-*exo* cyclization. A: Activation barriers *vs.* the incipient C···C distance of the forming bond in the TS. B: Activation barriers *vs.* reaction energies.

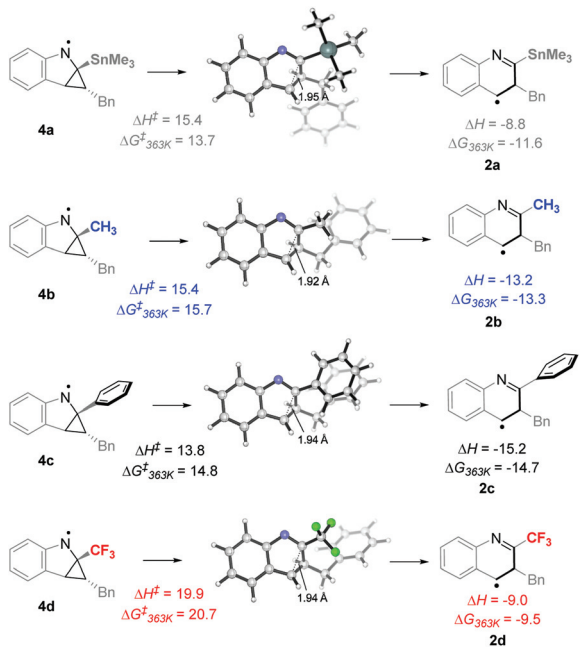

Scheme 10 Substrate comparison for retro 3-*exo* cyclization. Adjacent group can influence this step through steric or electronic effects (energies in kcal mol^{-1}).

The overall cascade surfaces. Although the tricyclic product of the 3-*exo*-trig cyclization **4b**/**4c** are slightly higher in energy than the 5-*exo*-product **3b**/**3c** (due to strain accumulation) and although the retro-3-*exo*-trig barrier for the conversion of **4b**/**4c** to the final 6-*endo* product **2c** was relatively high (15.6 kcal mol^{-1} relatively to **4b**/**4c**), the overall potential energy surface (PES) for the 5-*exo* → 6-*endo* HRE is much lower than the PES for the direct 6-*endo*-trig closure (Scheme 11 and ESI†).

Most interestingly, the combined PES reveals a clear difference of the Sn-mediated cascade from that of the three C-centered radicals. Because the first 5-*exo*-trig cyclization is considerably less exergonic for the Sn-case, the absolute energies of the HRE transition states are quite close to the 5-*exo* TS energy (Scheme 12). As a consequence, the retro-3-*exo* step is predicted to be the rate-limiting step for the Me_3Sn-mediated cascade (*i.e.*, the present model system). Although we could not model the full $SnBu_3$-substituted system, the large steric bulk of this substituent (which can be called "an oversized *t*-Bu group") strongly suggests that even the 1st step of the HRE sequence should be decelerated so much that ring expansion is slower than the intermolecular H-abstraction, *i.e.*, the path that delivers the experimentally observed 5-*exo*-trig products.

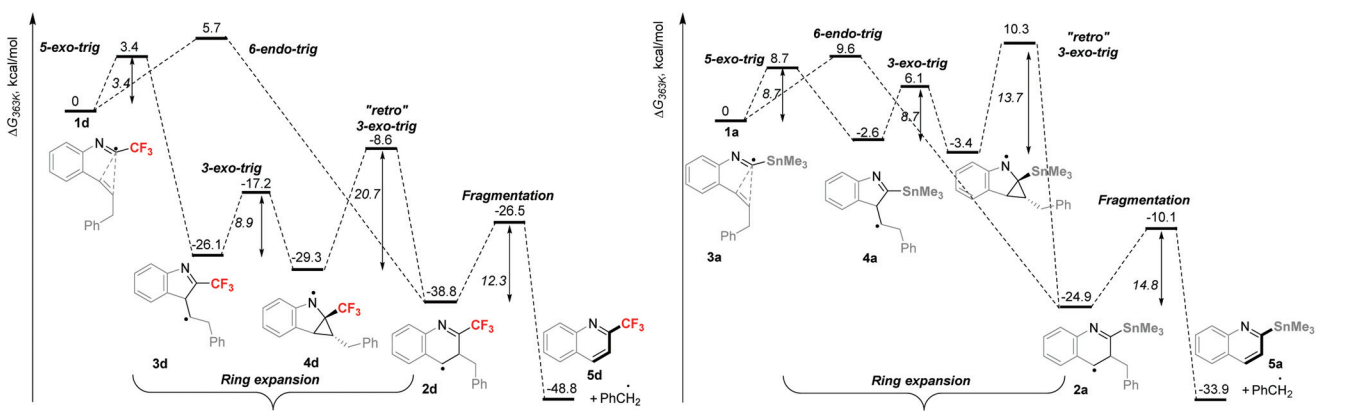

Scheme 11 Gibbs Free Energy diagram for full radical cascade initiated by the addition of the CF_3 and $SnMe_3$ radicals, including HRE, direct 6-*endo* path and fragmentation. See ESI† for the other full cascade PESs.

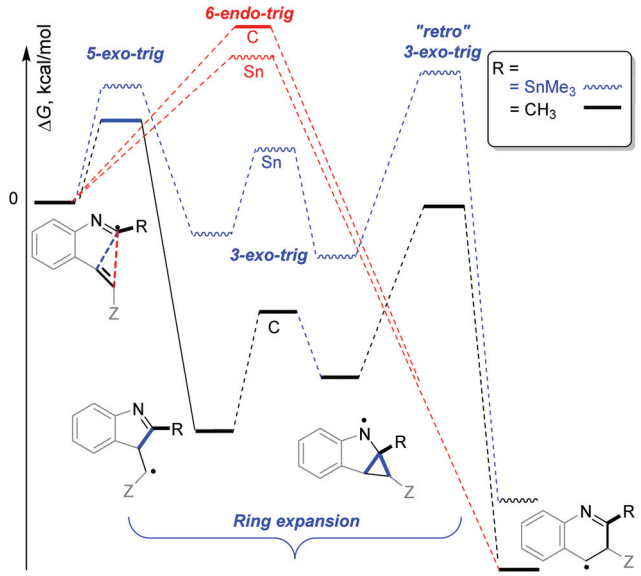

Scheme 12 Taking the path of least resistance – the multistep indirect "all-*exo*" route can be the lowest energy path to an *endo*-cyclization product. The *endo*-trig paths are shown in red. The HRE path for Me-substituted radicals (used to illustrate the trend for all C-centered radicals cascades) is shown in black, the HRE path for the Sn-substituted system is shown in blue.

The contrast between the carbon-radical and Sn-radical mediated cascades can be further illustrated by the following – it would take 13–21 kcal mol^{-1} to raise the 3-*exo*-TS to the same absolute energy as the 5-*exo*-TS (the point where half of the 5-*exo*-product would revert back in the absence of external H-atom trapping) whereas the difference between these barriers is >3 kcal mol^{-1} for the Sn-cascade.

Conclusions

Analysis of the calculated potential energy surfaces for the full HRE/fragmentation cascades reiterates the importance of stereoelectronic concepts in the design of cyclization processes. Even though the direct 6-*endo* cyclization is not as disfavored as its 4-*endo* and 5-*endo* cousins, the combination of three *exo*-cyclizations (*i.e.*, the 5-*exo*/homoallylic expansion) is still energetically preferred over the "direct" *endo* path to the six-membered product (Scheme 12). Avoiding the direct path in favor of a combination of indirect multi-step route is reminiscent of the commonly encountered situation in catalysis when an unfavorable single-step transformation is accomplished in a more favorable way *via* a combination of elementary steps enabled by substrate/catalyst interactions.[25] This is a manifestation of the general *exo*-trig preference for cyclizations.[21]

Electron acceptor substitution, such as the CF_3 group, can facilitate the 6-*endo*-trig ring closure but the *exo*-path still remains the preferred path for the group of substituents investigated in the present work. On the other hand, the effect of structural constraints on the 5-*exo*/6-*endo* competition is more complex and it is possible to guide this transformation directly down the 6-*endo* path by annealing additional cycles to the alkene.

Most interestingly, the Sn-radical mediated potential energy surface is significantly different from that for the C-radical mediated processes. Because the first 5-*exo* step of the cascade is only weakly exergonic, the subsequent strained transition states for the ring expansion steps are much closer in the absolute energy to the first TS. The large differences in the calculated PES should be related to the large differences in the experimentally observed reaction selectivities for the Sn- and C-radical mediated processes.

In summary, this work presents a comprehensive experimental and theoretical study of radical cascades that transform *o*-alkenylarylisonitriles into substituted quinolones. The shapes of the multistep potential energy surfaces originating from the reaction of substituted imidoyl radicals depend strongly on the nature of these "bystander" substituents. Whereas cascades initiated by the addition of carbon-centered radicals proceed through a highly exothermic first ring closure that is clearly the rate-determining step, the 5-*exo*-trig cyclization of Sn-substituted radicals is closer to thermoneutrality and thus can be reversible, if other steps of the homoallylic cascade have higher barriers. The combination of chemoselective radical additions to isonitriles with an alkene partner equipped with appropriate scissile "weak link" allows for an efficient sequence of steps leading to the *de novo* assembly of the substituted quinoline core. This is a new way for using alkenes as synthetic equivalents to alkynes.

Acknowledgements

This study was supported by the National Science Foundation (Grant CHE-1465142). We are also grateful to NSF XSEDE (TG-CHE160006) and RCC FSU for computational resources. G. d. P. G. is grateful to IBM for the 2016 IBM Ph.D Scholarship.

References

1 Selected examples: M. Newcomb, A. G. Glenn and W. G. Williams, *J. Org. Chem.*, 1989, **54**, 2675; A. L. J. Beckwith and V. W. Bowry, *J. Org. Chem.*, 1989, **54**, 2681; N. F. O'Rourke, K. A. Davies and J. E. Wulff, *J. Org. Chem.*, 2012, **77**, 8634 Related ring expansions: Dowd-Beckwith – P. Dowd and S. C. Choi, *J. Am. Chem. Soc.*, 1987, **109**, 3493; P. Dowd and S. C. Choi, *J. Am. Chem. Soc.*, 1987, **109**, 6548; A. L. J. Beckwith, D. M. O'Shea and S. W. Westwood, *J. Am. Chem. Soc.*, 1988, **110**, 2565; C. Wang, X. Gu, M. S. Yu and D. P. Curran, *Tetrahedron*, 1998, **54**, 8355 Neophyl – J. T. Banks and J. C. Scaiano, *J. Phys. Chem.*, 1995, **99**, 3527; R. L. Donkers and M. S. Workentin, *J. Am. Chem. Soc.*, 2004, **126**, 1688;

D. E. Falvey, B. S. Khambatta and G. B. Schuster, *J. Phys. Chem.*, 1990, **94**, 1056; M. Bietti and M. Salamone, *J. Org. Chem.*, 2005, **70**, 10603; K. U. Ingold, M. Smeu and G. A. DiLabio, *J. Org. Chem.*, 2006, **71**, 9906; A. Baroudi, J. Alicea, P. Flack, J. Kirincich and I. V. Alabugin, *J. Org. Chem.*, 2011, **76**, 1521.

2 (*a*) G. Stork and R. Mook Jr., *Tetrahedron Lett.*, 1986, **27**, 4529; (*b*) A. L. J. Beckwith and D. M. O'Shea, *Tetrahedron Lett.*, 1986, **27**, 4525.

3 (*a*) S. Mondal, B. Gold, R. K. Mohamed and I. V. Alabugin, *Chem. – Eur. J.*, 2014, **20**, 8664; (*b*) S. Mondal, B. Gold, R. Mohamed, H. Phan and I. V. Alabugin, *J. Org. Chem.*, 2014, **79**, 7491; (*c*) R. K. Mohamed, S. Mondal, B. Gold, C. J. Evoniuk, T. Banerjee, K. Hanson and I. V. Alabugin, *J. Am. Chem. Soc.*, 2015, **137**, 6335; (*d*) R. K. Mohamed, S. Mondal, J. V. Guerrera, T. M. Eaton, T. E. Albrecht-Schmitt, M. Shatruk and I. V. Alabugin, *Angew. Chem., Int. Ed.*, 2016, **55**, 12054.

4 I. V. Alabugin and M. Manoharan, *J. Am. Chem. Soc.*, 2005, **127**, 12583.

5 (*a*) C. J. Evoniuk, M. Ly and I. V. Alabugin, *Chem. Commun.*, 2015, **51**, 12831; (*b*) C. J. Evoniuk, G. P. Gomes, M. Ly, F. D. White and I. V. Alabugin, *J. Org. Chem*, DOI: 10.1021/acs.joc.7b00262.

6 5-*exo*-radical-cyclizations of *o*-alkenyl arylisocyanides with organotin reagents: (*a*) S. Kobayashi, G. Peng and T. Fukuyama, *Tetrahedron Lett.*, 1999, **40**, 1519; (*b*) M. Kotani, S. Yamago, A. Satoh, H. Tokuyama and T. Fukuyama, *Synlett*, 2005, 1893; (*c*) T. Fukuyama, X. Chen and G. Peng, *J. Am. Chem. Soc.*, 1994, **116**, 3127; (*d*) H. Tokuyama and T. Fukuyama, *Chem. Rec.*, 2002, **2**, 37.

7 (*a*) W. C. Danen and C. T. West, *J. Am. Chem. Soc.*, 1973, **95**, 6872; (*b*) H. Yan, G. Rong, D. Liu, Y. Zheng, J. Chen and J. Mao, *Org. Lett.*, 2014, **16**, 6306.

8 For work involving boronic acids as radical precursors: (*a*) M. Tobisu, K. Koh, T. Furukawa and N. Chatani, *Angew. Chem., Int. Ed.*, 2012, **51**, 11363; (*b*) M. Heinrich and A. Gansäuer, *Radicals in Synthesis III*, Springer Science & Business Media, 2012; (*c*) J. W. Lockner, D. D. Dixon, R. Risgaard and P. S. Baran, *Org. Lett.*, 2011, **13**, 5628; (*d*) G. Yan, M. Yang and X. Wu, *Org. Biomol. Chem.*, 2013, **11**, 7999.

9 Mn-Mediated reactions of boronic acids: (*a*) G. Yan, M. Yang and X. Wu, *Org. Biomol. Chem.*, 2013, **11**, 7999; (*b*) A. S. Demir, Ö. Reis and M. Emrullahoglu, *J. Org. Chem.*, 2002, **68**, 578.

10 Formation of a carbon-centered radical in the reaction of Mn(III) and boronic acid: (*a*) A. S. Demir, Ö. Reis and M. Emrullahoglu, *J. Org. Chem.*, 2003, **68**, 578; (*b*) J. B. Bush and H. Finkbeiner, *J. Am. Chem. Soc.*, 1968, **90**, 5903; (*c*) E. I. Heiba, R. M. Dessau and W. J. Koehl, *J. Am. Chem. Soc.*, 1968, **90**, 5905; (*d*) B. B. Snider, *Chem. Rev.*, 1996, **96**, 339.

11 This selectivity provides an interesting contrast to reactions *via* the initially formed 5-*exo*-product is quickly intercepted by deprotonation/electron transfer. (*a*) A. Studer and D. P. Curran, *Nat. Chem.*, 2014, **6**, 765; (*b*) D. Leifert and A. Studer, *Angew. Chem., Int. Ed.*, 2016, **55**, 11660.

12 5-*exo*-cyclizations of *o*-alkenylarylisocyanides: (*a*) B. Zhang and A. Studer, *Org. Lett.*, 2014, **16**, 1216; (*b*) T. Mitamura, K. Iwata and A. Ogawa, *J. Org. Chem.*, 2011, **76**, 3880; (*c*) D. Leifert, D. G. Artiukhin, J. Neugebauer, A. Galstyan, C. A. Strassert and A. Studer, *Chem. Commun.*, 2016, **52**, 5997; (*d*) W. R. Bowman, A. J. Fletcher, P. J. Lovell and J. M. Pedersen, *Synlett*, 2004, 1905; (*e*) Palladium-catalyzed analog: M. Tobisu, H. Fujihara, K. Koh and N. Chatani, *J. Org. Chem.*, 2010, **75**, 4841.

13 M. J. Frisch, *et al.*, *Gaussian 09, Revision D.01*, Gaussian, Wallingford, CT, 2009. Complete reference in the ESI.†

14 (*a*) Y. Zhao and D. G. Truhlar, *Theor. Chem. Acc.*, 2008, **120**, 215; (*b*) Y. Zhao and D. G. Truhlar, *Acc. Chem. Res.*, 2008, **41**, 157.

15 Use of this functional in radical processes: (*a*) Y. Zhao and D. G. Truhlar, *J. Phys. Chem. A*, 2008, **112**, 1095. Selected example from our group: (*b*) K. Pati, G. P. Gomes, T. Harris, A. Hughes, H. Phan, T. Banerjee, K. Hanson and I. V. Alabugin, *J. Am. Chem. Soc.*, 2015, **137**, 1165; (*c*) T. Harris, G. P. Gomes, R. Clark and I. V. Alabugin, *J. Org. Chem.*, 2016, **81**, 6007; (*d*) K. Pati, G. Gomes and I. V. Alabugin, *Angew. Chem., Int. Ed.*, 2016, **55**, 11633 Other examples: (*e*) J. K. Lee and D. J. Tantillo, *Annu. Rep. Prog. Chem., Sect. B: Org. Chem.*, 2010, **106**, 283; (*f*) R. S. Paton, J. L. Mackey, W. H. Kim, J. H. Lee, S. J. Danishefsky and K. N. Houk, *J. Am. Chem. Soc.*, 2010, **132**, 9335–9340; (*g*) O. Gutierrez, J. C. Tellis, D. N. Primer, G. A. Molander and M. C. Kozlowski, *J. Am. Chem. Soc.*, 2015, **137**, 4896; (*h*) J.-F. Müller, Z. Liu, V. S. Nguyen, T. Stavrakou, J. N. Harvey and J. Peeters, *Nat. Commun.*, 2016, **7**, 13213; (*i*) A. Galano and J. R. Alvarez-Idaboy, *J. Comput. Chem.*, 2014, **35**, 2019; (*j*) J. M. Um, O. Gutierrez, F. Schoenebeck, K. N. Houk and D. W. C. MacMillan, *J. Am. Chem. Soc.*, 2010, **132**, 6001.

16 The Def2-QZVP basis set for Sn was obtained at Basis Set Exchange (https: //bse.pnl.gov/bse/portal): (*a*) D. Feller, *J. Comput. Chem.*, 1996, **17**, 1571; (*b*) K. L. Schuchardt, B. T. Didier, T. Elsethagen, L. Sun, V. Gurumoorthi, J. Chase, J. Li and T. L. Windus, *J. Chem. Inf. Model.*, 2007, **47**, 1045; (*c*) Reference for the basis set: F. Weigend and R. Ahlrichs, *Phys. Chem. Chem. Phys.*, 2005, **7**, 3297.

17 J. Tomasi, B. Mennucci and E. Cancès, *J. Mol. Struct. (THEOCHEM)*, 1999, **464**, 211.

18 (*a*) F. Weinhold, C. R. Landis and E. D. Glendening, *Int. Rev. Phys. Chem.*, 2016, **35**, 1; A. E. Reed and F. J. Weinhold, *Chem. Phys.*, 1985, **83**, 1736; (*b*) A. E. Reed and F. Weinhold, *Isr. J. Chem.*, 1991, **31**, 277; (*c*) A. E. Reed, L. A. Curtiss and F. Weinhold, *Chem. Rev.*, 1988, **88**, 899; (*d*) F. Weinhold, in *Encyclopedia of Computational Chemistry*, ed. P.v.R. Schleyer, Wiley, New-York, 1998, vol. 3, p. 1792. Selected recent applications of NBO analysis towards analysis of organic structure and reactivity: J. Podlech, *J. Phys. Chem. A*, 2010, **114**, 8480; M. P. Freitas, *J. Org. Chem.*, 2012, **77**, 7607; K. T. Greenway, A. G. Bischoff

and B. M. Pinto, *J. Org. Chem.*, 2012, **77**, 9221; (*e*) D. Vidhani, M. Krafft and I. V. Alabugin, *J. Am. Chem. Soc.*, 2016, **138**, 2769; (*f*) E. Juaristi and R. Notario, *J. Org. Chem.*, 2015, **80**, 2879; (*g*) G. P. Gomes, V. Vil', A. Terent'ev and I. V. Alabugin, *Chem. Sci.*, 2015, **6**, 6783; (*h*) E. Juaristi and R. Notario, *J. Org. Chem.*, 2016, **81**, 1192; (*i*) G. P. Gomes, I. A. Yaremenko, P. S. Radulov, R. A. Novikov, V. V. Chernyshev, A. A. Korlyukov, G. I. Nikishin, I. V. Alabugin and A. O. Terent'ev, *Angew. Chem., Int. Ed.*, in print.

19 The bent geometry at both the N and the C centers of the imidoyl radical is associated with the penalty for rehybridization. Although the linear geometry would maximize the stabilizing effect of 3e-interaction between the lone pair and the radical, achieving this geometry would compromise preferred hybridization states of the two centers. For example, the penalty for linearizing the vinyl radical was estimated to be ~5 kcal mol^{-1} by Nicolaides and Borden: A. Nicolaides and W. T. Borden, *J. Am. Chem. Soc.*, 1991, **113**, 6750. For a more general discussion of rehybridization effects, see: I. V. Alabugin, S. Bresch and G. P. Gomes, *J. Phys. Org. Chem.*, 2015, **28**, 147 For a more specific discussion of electronic effects at nitrogen, see: I. V. Alabugin, M. Manoharan, M. Buck and R. Clark, *THEOCHEM*, 2007, **813**, 21; I. V. Alabugin, S. Bresch and M. Manoharan, *J. Phys. Chem. A*, 2014, **118**, 3663; W. T. Borden, *J. Phys. Chem. A*, 2017, **121**, 1140.

20 Note that, upon this rotation, the apparent electronic character of imidoyl moiety to the terminal aromatic system can change from a $\pi^*_{C=N}$ acceptor to a 2c,3e-donor, suggesting chameleonic properties of imidoyl radicals. S. Z. Vatsadze, Y. D. Loginova, G. Gomes and I. V. Alabugin, *Chem. – Eur. J.*, 2016, **23**, 3225.

21 I. V. Alabugin, *Stereoelectronic Effects: The Bridge between Structure and Reactivity*, John Wiley & Sons Ltd, Chichester, UK, 2016.

22 (*a*) I. V. Alabugin and K. Gilmore, *Chem. Commun.*, 2013, **49**, 11246; (*b*) K. Gilmore, R. K. Mohamed and I. V. Alabugin, The Baldwin Rules: Revised and Extended, *Wiley Interdiscip. Rev.: Comput. Mol. Sci.*, 2016, **6**, 487.

23 S. F. Vasilevsky, B. Gold, T. F. Mikhailovskaya and I. V. Alabugin, *J. Phys. Org. Chem.*, 2012, **25**, 998.

24 Z.-W. Hou, Z.-Y. Mao, H.-B. Zhao, Y. Y. Melcamu, X. Lu, J. Song and H.-C. Xu, *Angew. Chem., Int. Ed.*, 2016, **55**, 9168.

25 D. J. Tantillo, *Acc. Chem. Res.*, 2016, 741.